JACS
JOURNAL OF THE AMERICAN CHEMICAL SOCIETY
Article
pubs.acs.org/JACS

# Giant Piezoelectricity in Potassium–Sodium Niobate Lead-Free Ceramics

Xiaopeng Wang,[†] Jiagang Wu,*[,†] Dingquan Xiao,[†] Jianguo Zhu,[†] Xiaojing Cheng,[†] Ting Zheng,[†] Binyu Zhang,[†] Xiaojie Lou,[‡] and Xiangjian Wang[‡]

[†]Department of Materials Science, Sichuan University, Chengdu 610064, People's Republic of China

[‡]Multi-disciplinary Materials Research Center, Frontier Institute of Science and Technology, and State Key Laboratory for Mechanical Behavior of Materials, Xi'an Jiaotong University, Xi'an 710049, People's Republic of China

**ABSTRACT:** Environment protection and human health concern is the driving force to eliminate the lead from commercial piezoelectric materials. In 2004, Saito et al. [Saito et al., *Nature*, **2004**, *432*, 84.] developed an alkali niobate-based perovskite solid solution with a peak piezoelectric constant $d_{33}$ of 416 pC/N when prepared in the textured polycrystalline form, intriguing the enthusiasm of developing high-performance lead-free piezoceramics. Although much attention has been paid on the alkali niobate-based system in the past ten years, no significant breakthrough in its $d_{33}$ has yet been attained. Here, we report an alkali niobate-based lead-free piezoceramic with the largest $d_{33}$ of ~490 pC/N ever reported so far using conventional solid-state method. In addition, this material system also exhibits excellent integrated performance with $d_{33}$~390–490 pC/N and $T_C$~217–304 °C by optimizing the compositions. This giant $d_{33}$ of the alkali niobate-based lead-free piezoceramics is ascribed to not only the construction of a new rhombohedral–tetragonal phase boundary but also enhanced dielectric and ferroelectric properties. Our finding may pave the way for "lead-free at last".

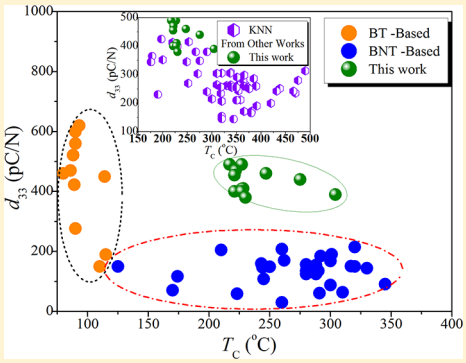


## INTRODUCTION

High-performance piezoceramics are one special class of functional materials and have been widely used in modern electronic devices. The research on these kinds of materials has always been hot and a new frontier in the scientific community.[1] Since the 1950s, $PbZr_{1-x}Ti_xO_3$ (PZT)-based ceramics have drawn much attention because of their excellent piezoelectric properties. As a consequence, they have been extensively utilized in almost all kinds of piezoelectric devices.[2] However, the more than 60% toxic lead element in PZT exerts pressure on the surrounding environment during their preparation and processing.[3,4] To maintain social sustainable development, many countries have paid much attention to the research and development of lead-free piezoelectric materials,[4−17] as a replacement to the lead-based ones.[18] As a result, there is an increasing interest in developing lead-free piezoelectrics with the aim of achieving an equivalent or even higher piezoelectric response as those of the lead-based ones.[3−23]

In 2004, Saito et al. reported a peak piezoelectric constant $d_{33}$ of 416 pC/N in the $Li^+$-, $Ta^{5+}$-, and $Sb^{5+}$-modified (K,Na)$NbO_3$ (KNN) textured ceramics using the reactive templated grain growth (RTGG) method.[19] E. Cross commented that such research will result in "lead-free at last" in the near future.[24] Since then, KNN has become one of the most extensively investigated lead-free piezoelectric systems in the past ten years [Figure 1a] because of its large $d_{33}$ and a high Curie temperature ($T_C$).[4,19−23,25−31] In order to further enhance its piezoelectric properties, recently a great amount of attention has been given to the phase transition of KNN by finely tailoring its composition [Figure 1b and c]. Constructing the orthorhombic–tetragonal phase coexistence has been the most popular approach to enhance the $d_{33}$ of KNN ceramics. However, $d_{33}$ obtained in this manner is still inferior or only comparable to that of the textured KNN-based ceramic reported by Satio et al. In 2010, Philip Ball[32] believed

> *there is no lack of other candidates, but none has yet been able to boast a $d_{33}$ comparable to that of PZT -until now.*

Therefore, it is of great importance to develop lead-free piezoceramics with high performance and show their promise in replacing the working horse PZT someday in the future.

It is well known that the rhombohedral and tetragonal (R–T) phase boundary of PZT ceramics brings up excellent piezoelectric properties;[33] that is, the piezoelectric properties are maximized in the vicinity of the structural phase transition line between R and T phases.[33] As a result, the aim of this work is to promote the $d_{33}$ of KNN-based ceramics by constructing the R–T phase boundary. In this work, we constructed a R–T phase boundary using the new material system of $(1-x)(K_{1-y}Na_y)(Nb_{1-z}Sb_z)O_3-xBi_{0.5}(Na_{1-w}K_w)_{0.5}ZrO_3$ ($0 \le x \le 0.05$, $0.40 \le y \le 0.68$, $0 \le z \le 0.08$, and $0 \le w \le 1$) via the conventional solid-state method. In this material system, adding $[Bi_{0.5}(Na_{1-w}K_w)_{0.5}]^{2+}$ and $Zr^{4+}$ could drop $T_{O-T}$ and raise $T_{R-O}$ of $(K_{1-y}Na_y)(Nb_{1-z}Sb_z)O_3$, respectively.[34] In addition, the

**Received:** January 9, 2014
**Published:** February 5, 2014

   dx.doi.org/10.1021/ja500076h | *J. Am. Chem. Soc.* 2014, 136, 2905–2910

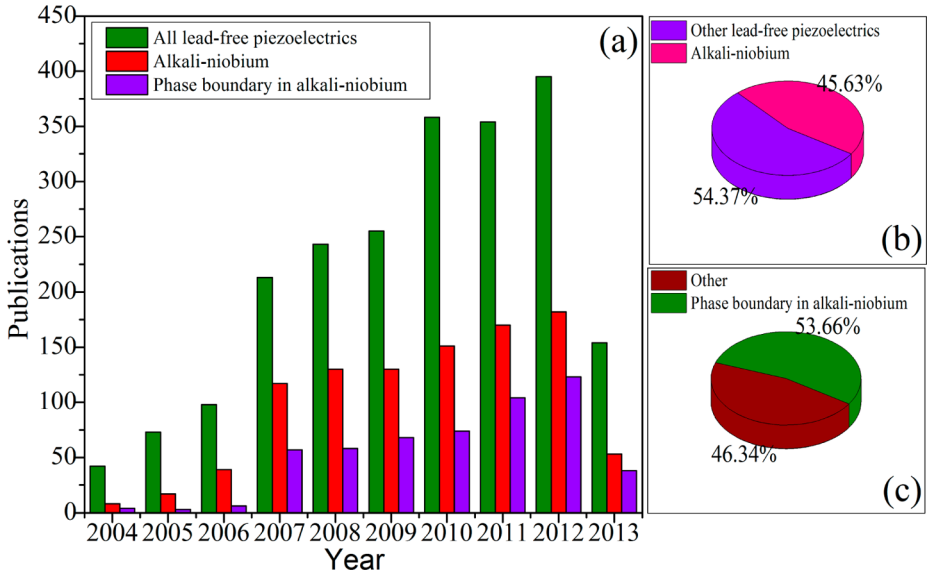


**Figure 1.** (a) Publications on lead-free piezoceramics in refereed journals for the time range from 2004 to July, 2013. The statistic is obtained from a "Web of Science" search with the keywords "lead-free" and "piezoelectric". (b) Publications on alkali-niobium piezoceramics/all lead-free piezoceramics. (c) Publications on alkali-niobium piezoceramics with and without the phase boundaries construction.

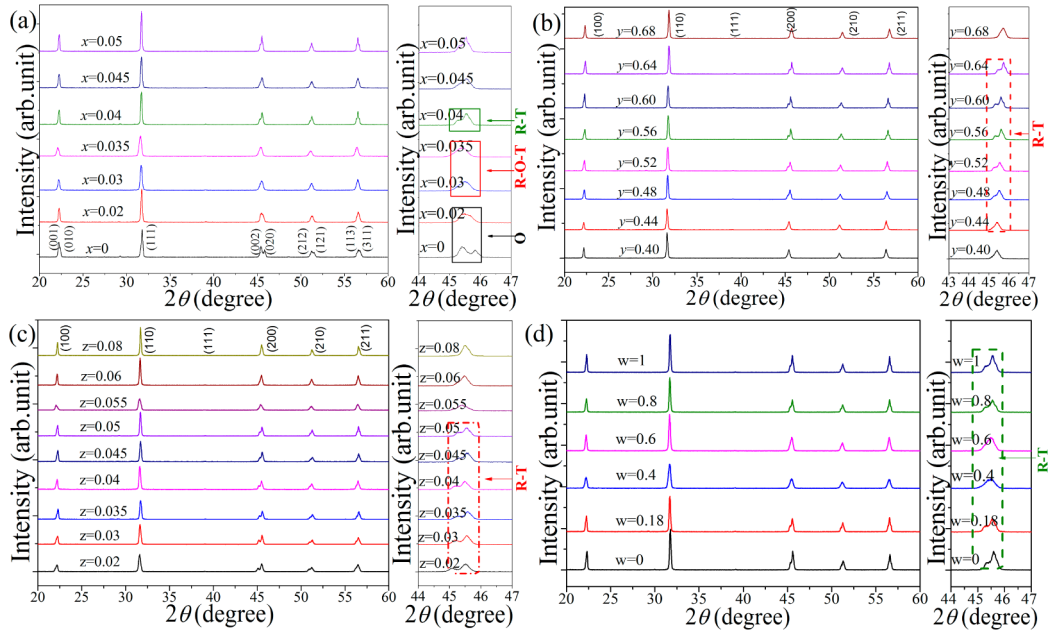


**Figure 2.** XRD patterns of the $(1-x)(K_{1-y}Na_y)(Nb_{1-z}Sb_z)O_3-xBi_{0.5}(Na_{1-w}K_w)_{0.5}ZrO_3$ ceramics with (a) $y = 0.52$, $z = 0.05$, $w = 0.18$, (b) $x = 0.04$, $z = 0.05$, $w = 0.18$, (c) $x = 0.04$, $y = 0.52$, $w = 0.18$, and (d) $x = 0.04$, $y = 0.52$, $z = 0.05$.

$Sb^{5+}$ substitution for $Nb^{5+}$ could stabilize the R−T phase coexistence. Indeed, we found that an R−T phase boundary can be constructed by optimizing the $x$, $y$, $z$, and $w$ of such a material system. A large $d_{33}$ of ∼490 pC/N has been obtained in the ceramics with the composition lying in the R−T phase boundary, which is superior to other results of KNN-based ceramics ever reported so far.

## ■. EXPERIMENTAL SECTION

$(1-x)(K_{1-y}Na_y)(Nb_{1-z}Sb_z)O_3-xBi_{0.5}(Na_{1-w}K_w)_{0.5}ZrO_3$ ($0 \le x \le 0.05$, $0.40 \le y \le 0.68$, $0 \le z \le 0.08$, and $0 \le w \le 1$) lead-free piezoceramics were prepared by using the conventional solid-state method, and the raw materials were $K_2CO_3$, $ZrO_2$, $Nb_2O_5$, $Bi_2O_3$, $Na_2CO_3$, and $Sb_2O_3$. The synthesis procedure was described in our previous literature.[6,21,23,34] All disk samples were sintered at 1060−1150 °C for 3 h in air, and a *dc* field of 3.0−4.0 kV/mm was used to pole all samples at 30 °C in a silicone oil bath. X-ray diffraction (XRD) (DX2700, Dandong, China) was employed to detect the structural properties of the samples. The curves of the capacitance against temperatures of the sintered samples were characterized using an *LCR* analyzer (HP 4980, Agilent, U. S. A.). A quasistatic $d_{33}$ meter (ZJ-3A, Institute of Acoustics, Chinese Academy of Sciences, China) and an impedance analyzer (HP 4294A, Agilent, U. S. A.) were used to characterize the piezoelectric constant ($d_{33}$) and the electromechanical coupling factor ($k_p$) according to the IEEE standards.


dx.doi.org/10.1021/ja500076h | J. Am. Chem. Soc. 2014, 136, 2905−2910

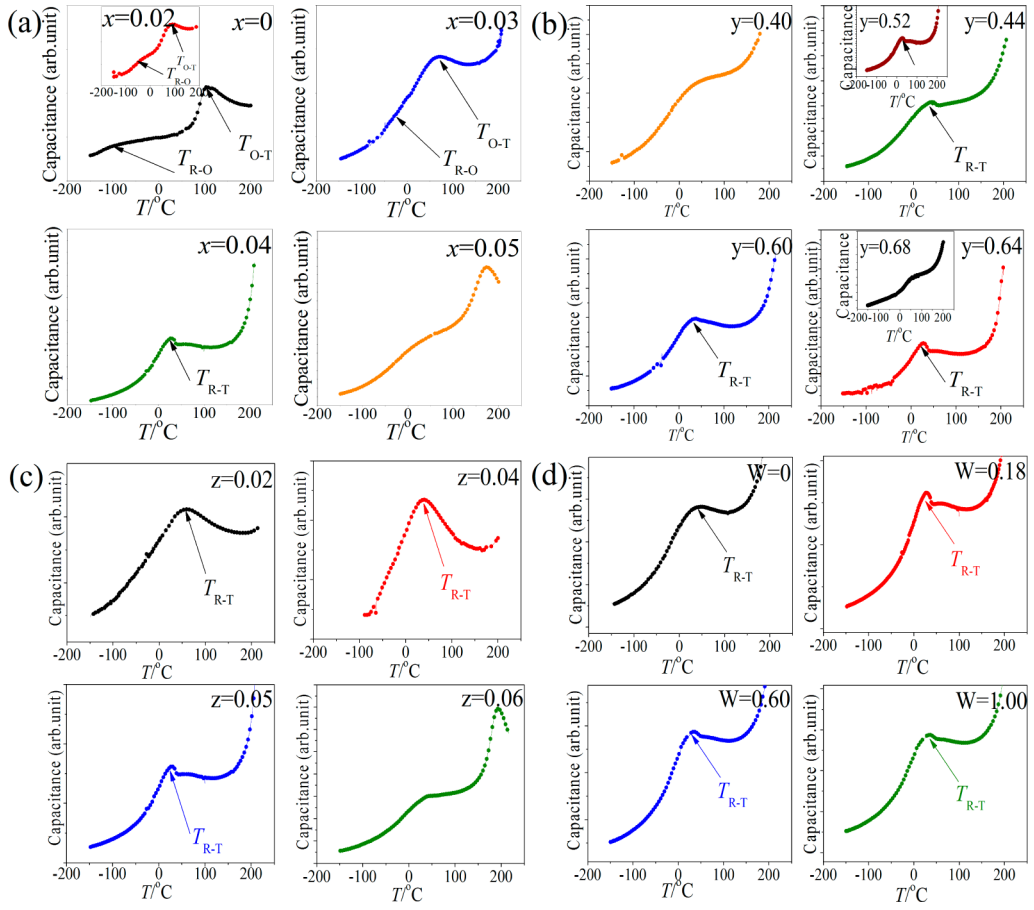


**Figure 3.** Temperature-dependent capacitance of the $(1-x)(K_{1-y}Na_y)(Nb_{1-z}Sb_z)O_3 - xBi_{0.5}(Na_{1-w}K_w)_{0.5}ZrO_3$ ceramics with (a) $y = 0.52$, $z = 0.05$, $w = 0.18$, (b) $x = 0.04$, $z = 0.05$, $w = 0.18$, (c) $x = 0.04$, $y = 0.52$, $w = 0.18$, and (d) $x = 0.04$, $y = 0.52$, $z = 0.05$ measured at 10 kHz and in the temperature range of −150−200 °C.

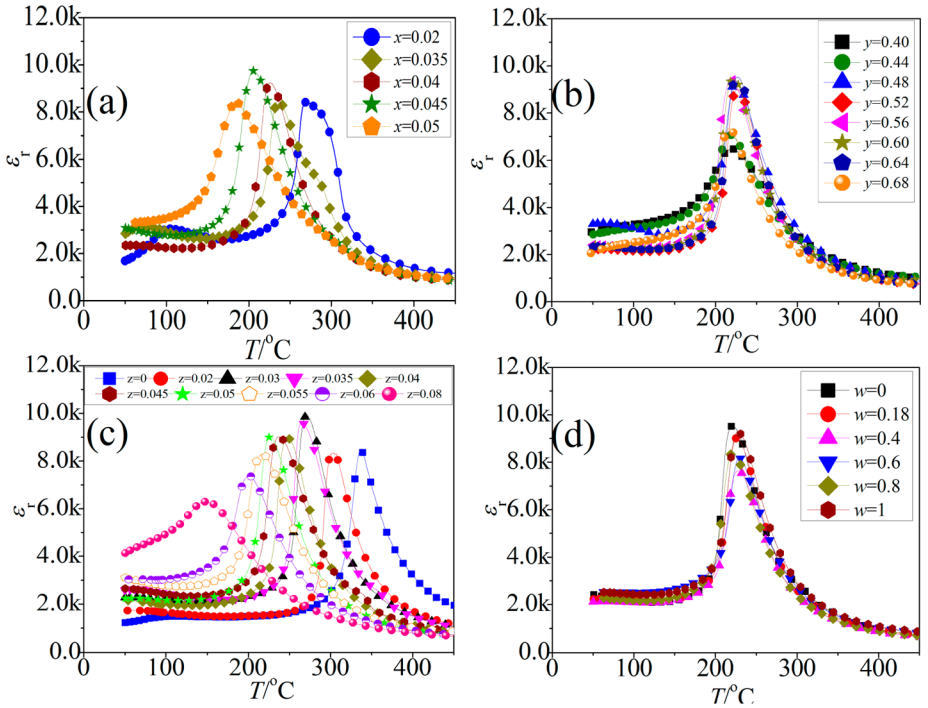


**Figure 4.** (a) $\varepsilon_r$ plotted against temperatures of the $(1-x)(K_{1-y}Na_y)(Nb_{1-z}Sb_z)O_3 - xBi_{0.5}(Na_{1-w}K_w)_{0.5}ZrO_3$ ceramics with (a) $y = 0.52$, $z = 0.05$, $w = 0.18$, (b) $x = 0.04$, $z = 0.05$, $w = 0.18$, (c) $x = 0.04$, $y = 0.52$, $w = 0.18$, and (d) $x = 0.04$, $y = 0.52$, $z = 0.05$.


dx.doi.org/10.1021/ja500076h | J. Am. Chem. Soc. 2014, 136, 2905−2910

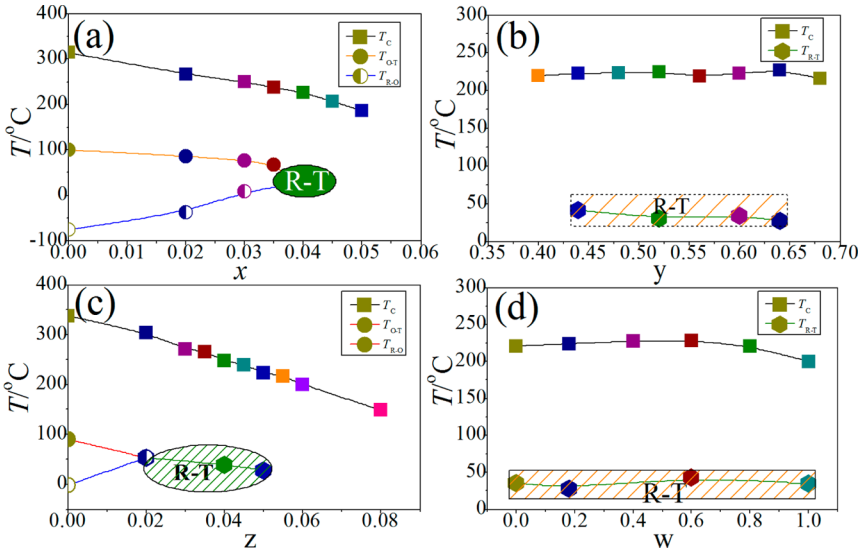


**Figure 5.** Phase diagram of the $(1-x)(K_{1-y}Na_y)(Nb_{1-z}Sb_z)O_3-xBi_{0.5}(Na_{1-w}K_w)_{0.5}ZrO_3$ ceramics with (a) $y = 0.48$, $z = 0.05$, $w = 0.18$; (b) $x = 0.04$, $z = 0.05$, $w = 0.18$; (c) $x = 0.04$, $y = 0.48$, $w = 0.18$; (d) $x = 0.04$, $y = 0.48$, $z = 0.05$.

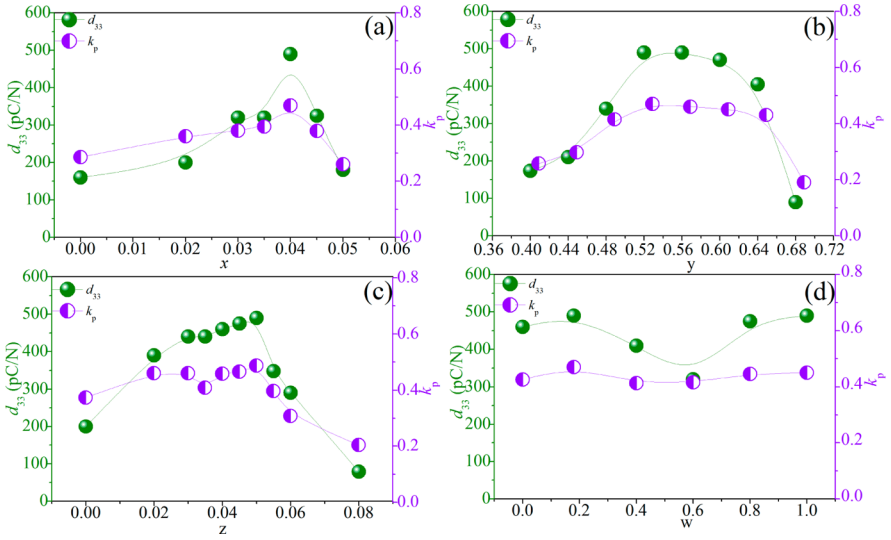


**Figure 6.** $d_{33}$ and $k_p$ of the $(1-x)(K_{1-y}Na_y)(Nb_{1-z}Sb_z)O_3-xBi_{0.5}(Na_{1-w}K_w)_{0.5}ZrO_3$ ceramics with (a) $y = 0.52$, $z = 0.05$, $w = 0.18$; (b) $x = 0.04$, $z = 0.05$, $w = 0.18$; (c) $x = 0.04$, $y = 0.52$, $w = 0.18$; (d) $x = 0.04$, $y = 0.52$, $z = 0.05$.

## ■. RESULTS AND DISCUSSION

Figure 2 shows the XRD patterns of the $(1-x)(K_{1-y}Na_y)(Nb_{1-z}Sb_z)O_3-xBi_{0.5}(Na_{1-w}K_w)_{0.5}ZrO_3$ ceramics as a function of $x$, $y$, $z$, and $w$. A pure perovskite phase without secondary phases was obtained in all the samples. As shown in Figure 2a, an orthorhombic phase is evidently observed in the ceramics with $0 \le x \le 0.02$, and the rhombohedral (R), orthorhombic (O), and tetragonal (T) phases were found to coexist for the composition of $0.02 < x \le 0.035$. As $x$ further increases, the ceramics with $0.035 < x < 0.045$ show mixed R and T phases, confirmed by the temperature-dependent dielectric measurements shown in Figure 3a. Figure 3a show the capacitance of these ceramics versus temperature (−150–200 °C), which could be used to identify the phase evolution of $T_{R-O}$ and $T_{O-T}$. Two phase transition peaks at $T_{R-O}$ and $T_{O-T}$ could be shown in the ceramics with $x = 0$, 0.02, and 0.03, and then they converge as the BNKZ content increases up to 0.04, leading to the formation of the R–T phase boundary. The R–T phase boundary is further suppressed as the BNKZ content increases up to 0.045. By using the similar analysis according to Figure 2b–d and 3b–d, the R–T phase coexistence has been achieved by optimizing the $y$, $z$, and $w$ of such a material system (i.e., $0.44 \le y \le 0.64$, $0.02 < z \le 0.05$, and $0 \le w \le 1$).

To check the effect of the $x$, $y$, $z$, and $w$ content on $T_C$, the temperature-dependent dielectric measurements were carried out on the ceramics at 10 kHz in a temperature range of 50–450 °C, and the results are shown in Figure 4a–d. The $T_C$ is dependent on the $x$, $y$, $z$, and $w$ content. For example, $T_C$ gradually descends as the $x$ increases, remains almost unchanged as $y$ varies, linearly decreases as the $z$ rises, and decreases for a higher K content in BNKZ. Figure 5a–d show the phase diagram of the $(1-x)(K_{1-y}Na_y)(Nb_{1-z}Sb_z)O_3-xBi_{0.5}(Na_{1-w}K_w)_{0.5}ZrO_3$ ceramics determined by both the XRD patterns and the dielectric properties against temperatures [see Figure 2–4]. We can see that the phase boundary is very sensitive to the composition of the material system. In those material systems, the addition of BNKZ can shift both $T_{O-T}$ and $T_{R-O}$ close to room temperature, which is similar to the


dx.doi.org/10.1021/ja500076h | J. Am. Chem. Soc. 2014, 136, 2905–2910

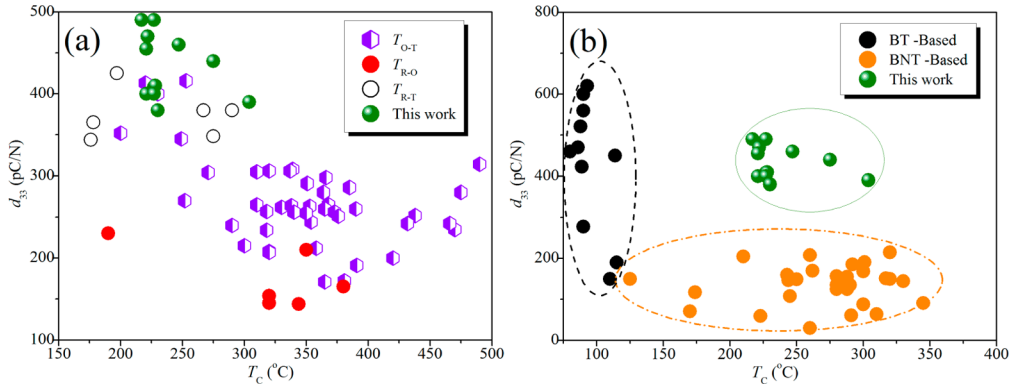


**Figure 7.** $d_{33}$ as a function of $T_C$ for (a) KNN-based piezoceramics and the $(1-x)(K_{1-y}Na_y)(Nb_{1-z}Sb_z)O_3 - xBi_{0.5}(Na_{1-w}K_w)_{0.5}ZrO_3$ ceramics developed in this work and (b) $Bi_{0.5}Na_{0.5}TiO_3$ (BNT)- and $BaTiO_3$ (BT)-based piezoceramics and the $(1-x)(K_{1-y}Na_y)(Nb_{1-z}Sb_z)O_3-xBi_{0.5}(Na_{1-w}K_w)_{0.5}ZrO_3$ ceramics developed in this work.

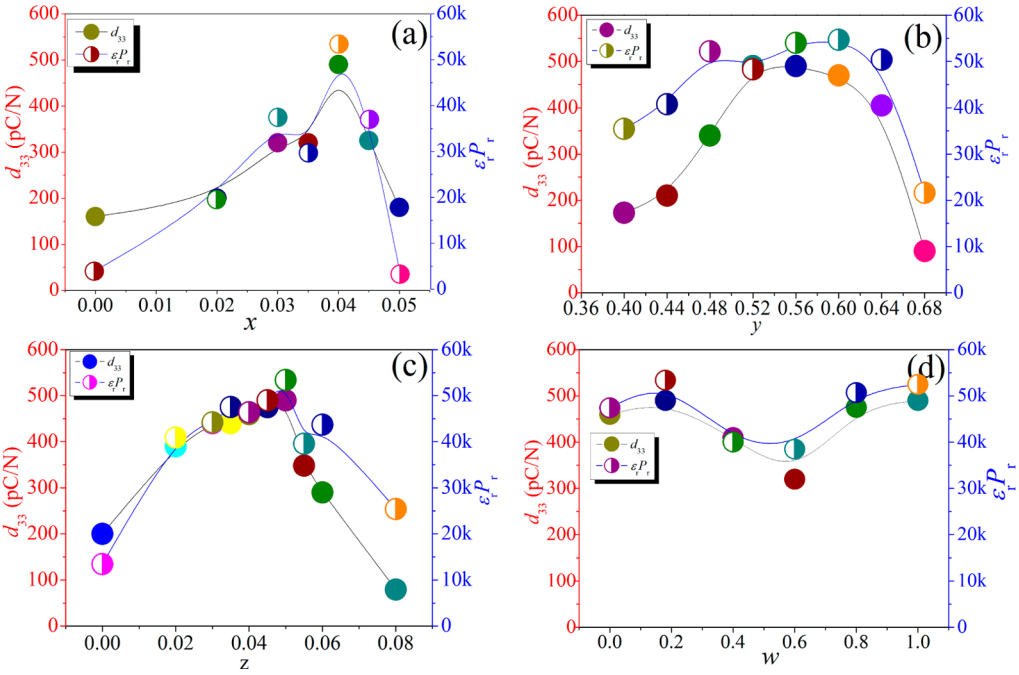


**Figure 8.** $\varepsilon_r P_r$ and $d_{33}$ of the $(1-x)(K_{1-y}Na_y)(Nb_{1-z}Sb_z)O_3-xBi_{0.5}(Na_{1-w}K_w)_{0.5}ZrO_3$ ceramics with (a) $y = 0.52$, $z = 0.05$, $w = 0.18$; (b) $x = 0.04$, $z = 0.05$, $w = 0.18$; (c) $x = 0.04$, $y = 0.52$, $w = 0.18$; (d) $x = 0.04$, $y = 0.52$, $z = 0.05$.

effect of $Sb^{5+}$.[35] The change in the K/Na ratio in KNNS also impacts on the phase structure [Figure 5b]. Finally, the R−T phase coexistence is achieved by optimizing the $x$, $y$, $z$, and $w$ of such a material system (i.e., $0.035 < x < 0.045$, $0.44 \le y \le 0.64$, $0.02 < z \le 0.05$, and $0 \le w \le 1$).

Figure 6a−d plot the $d_{33}$ and $k_p$ of the $(1-x)(K_{1-y}Na_y)(Nb_{1-z}Sb_z)O_3-xBi_{0.5}(Na_{1-w}K_w)_{0.5}ZrO_3$ ceramics. A $d_{33}$ of >400 pC/N has been obtained in the ceramics with $0.035 < x < 0.045$, $0.52 \le y \le 0.64$, $0.02 < z \le 0.05$, $0 \le w < 0.60$, and $0.60 < w \le 1$. Specifically, we can observe that the peak $d_{33}$ was found to be 490 pC/N with a $T_C$ of 227 °C for the $(1-x)(K_{1-y}Na_y)(Nb_{1-z}Sb_z)O_3-xBi_{0.5}(Na_{1-w}K_w)_{0.5}ZrO_3$ ceramic with $x = 0.04$, $y = 0.52$, $z = 0.05$, $w = 0.18$. Also, the $(1-x)(K_{1-y}Na_y)(Nb_{1-z}Sb_z)O_3-xBi_{0.5}(Na_{1-w}K_w)_{0.5}ZrO_3$ ceramic with $x = 0.04$, $y = 0.52$, $z = 0.03$, $w = 0.18$ shows a $d_{33}$ of 440 pC/N with a high $T_C$ of ∼275 °C, which are both superior to the result reported by Saito et al.[19] As a result, the $d_{33}$ of 390−490 pC/N and $T_C$ of 217−304 °C can be achieved by tuning the composition of these materials, indicating that the piezoelectric properties of the material system can be designed according to different application temperature ranges. To make a comparison of the $(1-x)(K_{1-y}Na_y)(Nb_{1-z}Sb_z)O_3-xBi_{0.5}(Na_{1-w}K_w)_{0.5}ZrO_3$ ceramics developed in this work with KNN and other lead-free piezoelectric materials, the $d_{33}$ as a function of $T_C$ are shown in Figure 7a and b. From Figure 7a, the $d_{33}$ obtained in this work is superior to other results on KNN-based ceramics reported so far.[4,7−31,35] The $d_{33}$ of the ceramics in this work could also compete with some of those PZT-based ceramics and are much higher than those nondoped PZT or other lead-free piezoceramics.[2] Because of the complex mixtures involved in such oxides, small changes in the composition may lead to considerable phase changes, giving rise to different piezoelectric behavior of the ceramics.[35−38] In this work, the giant $d_{33}$ is attributed to the enhanced polarizability induced by the coupling between two equivalent energy states of the tetragonal and rhombohedral phases.[35−38] Moreover, the equation of $d_{33} \sim \alpha \varepsilon_r P_r$ can show the relationship between dielectric and ferroelectric properties of a functional


dx.doi.org/10.1021/ja500076h | J. Am. Chem. Soc. 2014, 136, 2905−2910

material.[20,23] $\varepsilon_r P_r$ and $d_{33}$ against compositions of the $(1-x)(K_{1-y}Na_y)(Nb_{1-z}Sb_z)O_3-xBi_{0.5}(Na_{1-w}K_w)_{0.5}ZrO_3$ ceramics has been established, as shown in Figure 8. Interestingly, the similar trends of both $d_{33}$ and $\varepsilon_r P_r$ have been obtained in the studied material system. A peak for $d_{33}$ and $\varepsilon_r P_r$ has been simultaneously achieved for the ceramic with with the R and T phase boundary, confirming that the improved $\varepsilon_r P_r$ also plays a role on the giant $d_{33}$.

## ■. CONCLUSION

A giant $d_{33}$ (~490 pC/N) associated with the R–T phase boundary is first reported in alkali niobate-based system. In addition, the good comprehensive performance of $d_{33}$ and $T_C$ (e.g., $d_{33}$~390–490 pC/N and $T_C$~217–304 °C) could be induced by optimizing the composition of these materials. The good piezoelectric behavior is attributed to the formation of R–T phase boundary as well as enhanced dielectric and piezoelectric properties. We believe that the material system is a promising candidate as a replacement of lead-based piezoceramics in the near future.

## ■ AUTHOR INFORMATION


### Corresponding Author

* J. Wu. Email: msewujg@scu.edu.cn and wujiagang0208@163.com.


### Notes

The authors declare no competing financial interest.

## ■ ACKNOWLEDGMENTS

Authors gratefully acknowledge the supports of the National Science Foundation of China (NSFC nos. 51102173, 51272164, 51372195, and 51332003), the introduction of talent start funds of Sichuan University (2082204144033), and the Fundamental Research Funds for the Central Universities (2012SCU04A01).

## ■ REFERENCES


(1) Haertling, G. E. *J. Am. Ceram. Soc.* **1999**, *82*, 797.
(2) Jaffe, B.; Roth, R. S.; Marzullo, S. J. *Res. Natl Bur. Stand.* **1955**, *55*, 239.
(3) Takenaka, T.; Nagata, H. *Key Eng. Mater.* **1999**, *57*, 157.
(4) Rödel, J.; Jo, W.; Seifert, K. T. P.; Anton, E. M.; Granzow, T.; Damjanovic, D. *J. Am. Ceram. Soc.* **2009**, *92*, 1153.
(5) Liu, W.; Ren, X. *Phys. Rev. Lett.* **2009**, *103*, 257602.
(6) Wu, J.; Xiao, D.; Wu, W.; Chen, Q.; Zhu, J.; Yang, Z.; Wang, J. *Scr. Mater.* **2011**, *65*, 771.
(7) Zhang, S.; Xia, R.; Shrout, T. R. *J. Electroceram.* **2007**, *19* (4), 251.
(8) Matsubara, M.; Yamaguchi, T.; Kikuta, K.; Hirano, S. *Jpn. J. Appl. Phys. Part 1* **2005**, *44* (8), 6136.
(9) Damjanovic, D.; Klein, N.; Li, J.; Porokhonskyy, V. *Funct. Mater. Lett.* **2010**, *3*, 5.
(10) Zhu, F.; Skidmore, T. A.; Bell, A. J.; Comyn, T. P. C.; James, W.; Ward, M.; Milne, S. J. *Mater. Chem. Phys.* **2011**, *129*, 411.
(11) Wang, K.; Li, J. F. *Adv. Funct. Mater.* **2010**, *20*, 1924.
(12) Malic, B.; Bencan, A.; Rojac, T.; Kosec, M. *Acta. Chim. Slov.* **2008**, *55*, 719.
(13) Trodahl, H. J.; Klein, N.; Damjanovic, D.; Setter, N.; Ludbrook, B.; Rytz, D.; Kuball, M. *Appl. Phys. Lett.* **2008**, *93*, 262901.
(14) Hollenstein, E.; Damjanovic, D.; Setter, N. J. *Eur. Ceram. Soc.* **2007**, *27* (13–15), 4093.
(15) Wang, R.; Xie, R. J.; Hanada, K.; Matsusaki, K.; Kawanaka, H.; Bando, H.; Sekiya, T.; Itoh, M. *J. Electroceram.* **2008**, *21*, 263.
(16) Gupta, S.; Huband, S.; Keeble, D. S.; Walker, D.; Thomas, P.; Viehland, D.; Priya, S. *CrystEngComm* **2013**, *15*, 6790.
(17) Madaro, F.; Tolchard, J. R.; Yu, Y.; Einarsrud, M. A.; Grande, T. *CrystEngComm.* **2011**, *13*, 1350.
(18) EU-Directive 2002/95/EC. Off.. *J. Eur. Union* **2003**, *46* (L37), 19.
(19) Saito, Y.; Takao, H.; Tani, T.; Nonoyama, T.; Takatori, K.; Homma, T.; Nagaya, T.; Nakamura, M. *Nature* **2004**, *432*, 84.
(20) Shrout, T. R.; Zhang, S. J. *J. Electroceram.* **2007**, *19*, 111.
(21) Wu, J. G.; Wang, Y. Y.; Xiao, D. Q.; Zhu, J. G.; Yu, P.; Wu, L.; Wu, W. J. *Jpn. J. Appl. Phys.* **2007**, *46*, 7375.
(22) Guo, Y.; Kakimoto, K.; Ohsato, H. *Appl. Phys. Lett.* **2004**, *85*, 4121.
(23) Zhang, B. Y.; Wu, J. G.; Cheng, X. J.; Wang, X. P.; Xiao, D. Q.; Zhu, J. G.; Wang, X. J; Lou, X. J. *ACS Appl. Mater. Interface* **2013**, *5* (16), 7718.
(24) Cross, E. *Nature* **2004**, *432*, 24.
(25) Zhang, S.; Xia, R.; Shrout, T. R. *J. Electroceram.* **2007**, *19* (4), 251–257.
(26) Xiao, D. Q.; Wu, J. G.; Wu, L.; Zhu, J. G.; Yu, P.; Lin, D. M.; Liao, Y. W.; Sun, Y. *J. Mater. Sci.* **2009**, *44*, 5408.
(27) Hollenstein, E.; Davis, M.; Damjanovic, D.; Setter, N. *Appl. Phys. Lett.* **2005**, *87*, 182905.
(28) Klein, N.; Hollenstein, E.; Damjanovic, D.; Trodahl, H J.; Setter, N.; Kuball, M. *J. Appl. Phys.* **2007**, *102*, 014112.
(29) Lin, D.; Kwok, K. W.; Chan, H. L.W. *J. Appl. Phys.* **2007**, *102*, 034102.
(30) Wang, K.; Li, J. F.; Liu, N. *Appl. Phys. Lett.* **2008**, *93*, 092904.
(31) Akdogan, E. K.; Kerman, K.; Abazari, M.; Safari, A. *Appl. Phys. Lett.* **2008**, *92*, 112908.
(32) Philip, B. *Nat. Mater.* **2010**, *9*, 98.
(33) Jaffe, B.; Cook.; Jr., W. R.; Jaffe, H. Academic Press: New York, 1971.
(34) Wu, J. G.; Wang, X. P.; Cheng, X. J.; Xiao, D. Q.; Zhu, J. G. Patent (China) 201310392216.2, September 2, 2013.
(35) Zuo, R. Z.; Fu, J.; Lv, D. Y.; Liu, Y. *J. Am. Ceram. Soc.* **2010**, *93* (9), 2783.
(36) Ahart, M.; Somayazulu, M.; Cohen, R. E.; Ganesh, P.; Dera, P.; Mao, H. K.; Hemley, R. J.; Ren, Y.; Liermann, P.; Wu, Z. *Nature* **2008**, *451*, 545.
(37) Cohen, R. E. *Nature* **1992**, *358*, 136.
(38) Damjanovic, D. *Rep. Prog. Phys.* **1998**, *61*, 1267.